From heavy fermion antiferromagnetism to localized ferromagnetism: competition of two ground states in $CeRu_2Ge_2$ on cooling

1999 J. Phys.: Condens. Matter 11 5547

(http://iopscience.iop.org/0953-8984/11/29/301)

J. Phys.: Condens. Matter **11** (1999) 5547–5560. Printed in the UK PII: S0953-8984(99)02925-2

From heavy fermion antiferromagnetism to localized ferromagnetism: competition of two ground states in $CeRu_2Ge_2$ on cooling

S Raymond†‡, P Haen§, R Calemczuk‡, S Kambe‡, B Fåk‡, P Lejay§, T Fukuhara‡‖ and J Flouquet‡

† University of Geneva, DPMC, 24 quai E. Ansermet, 1211 Genève 4, Switzerland
‡ CEA—Grenoble, Département de Recherche Fondamentale sur la Matière Condensée, SPSMS, 38054 Grenoble Cédex, France
§ Centre de Recherche sur les Très Basses Températures, CNRS, BP 166, 38042 Grenoble Cédex, France
‖ Toyama Prefectural University, Toyama 939-03, Japan

Received 22 March 1999

Abstract. Resistivity, specific heat and neutron scattering measurements performed on single crystals of $CeRu_2Ge_2$ are reported. The intrinsic behaviour of this compound is to exhibit a double transition from a paramagnetic to an antiferromagnetic and then a ferromagnetic state on lowering the temperature with $T_N = 8.3$ K and respectively $T_C = 7.5$ K. For the first time the antiferromagnetic order is characterized by neutron scattering. The propagation vector of the sine-wave modulated structure is $\boldsymbol{k} = (0.31, 0, 0)$ as in the Si doped compounds. This phase is found to be easily weakened by disorder, but an antiferromagnetic moment as large as 1.5 μ_B develops between T_N and T_C for the best crystal.

1. Introduction

Heavy fermion compounds are located at the borderline of a magnetic instability and most often of an antiferromagnetic instability. This situation can be tuned by alloying or applying pressure on stoichiometric compounds. A quantum critical point (QCP) is reached for a vanishing Néel temperature. At the QCP, unusual behaviours of the resistivity and specific heat are linked to a dynamics controlled by an energy scale which is the temperature itself [1, 2]. In the vicinity of the QCP, antiferromagnetic correlations are a key feature demonstrated by neutron scattering measurements [3]. In this framework, an open question is the relevance of ferromagnetism which scarcely appears in these compounds. The proximity of a metamagnetic transition induced by applying a rather low magnetic field in some of these compounds indicates the importance of ferromagnetic coupling. In the extensively investigated system $CeRu_2Si_2$, a field of $H_m = 7.7$ T drives the compound from an enhanced Pauli paramagnetic state to a polarized state with strong anomalies in electronic, magnetic and lattice properties at the transition [4–6]. In a simple model based on the random phase approximation for the dynamical susceptibility used to analyse the inelastic neutron scattering data [7], ferromagnetic interactions were shown to develop above H_m on top of a vanishing local Kondo susceptibility [8]. Ferromagnetic interactions may also be relevant in zero field. More generally, in the CeM_2T_2 family (where M is a transition metal and T = Si or Ge), a common magnetic structure consists in antiferromagnetically coupled ferromagnetic sheets [9]. Most of these

0953-8984/99/295547+14$30.00

compounds crystallize in the $ThCr_2Si_2$ structure with the space group $I4/mmm$. Among them, $CeRu_2Ge_2$ is in a unique position, being a ferromagnet with $T_C \approx 8$ K. A challenge is to better understand the subtle balance between antiferromagnetic and ferromagnetic interactions in the CeM_2T_2 family. A parallel between the behaviour of $CeRu_2Si_2$ above H_m and the ground state of $CeRu_2Ge_2$ can be drawn. In particular this comparison can be based on the shape of the Fermi surface. In $CeRu_2Si_2$, the de Haas–van Alphen oscillations are interpreted in an itinerant model below H_m and in a localized model above H_m [10, 11]. In $CeRu_2Ge_2$, the Fermi surface is completely explained with a localized spin split model with some similarity with its counterpart $CeRu_2Si_2$ above H_m [12, 13]. Knowing that the RKKY interactions are directly linked to the shape of the Fermi surface this motivated us to investigate the intrinsic properties of $CeRu_2Ge_2$. In the past, it was shown that the behaviour of this compound is strongly sample dependent. A double transition was reported for polycrystalline samples [14, 15] but it was argued from a single crystal study that the second transition was not intrinsic [16]. The two transitions were ascribed to antiferromagnetic and ferromagnetic order, respectively [15, 17], while up to now neutron scattering experiments showed only ferromagnetic order and no attempt was made to search for an antiferromagnetic order [16, 18, 19]. Recently, other interest has grown in this compound thanks to works performed under high pressure and aiming to approach a QCP [20, 21, 22]. The magnetic instability is reached in this compound under an applied pressure of the order of 8.7 GPa and it is believed that it becomes the equivalent (from the point of view of the unit cell volume) of $CeRu_2Si_2$ at zero pressure for $P = 9.1$ GPa. The same phase diagram was investigated in the series of alloys $CeRu_2(Si_{1-x}Ge_x)_2$ [23, 24] where antiferromagnetic order is induced for $x > 0.05$ and the ground state becomes ferromagnetic for $x > 0.7$. The antiferromagnetic order, which corresponds in fact to a sine-wave modulated structure with the propagation vector $\boldsymbol{k} = (0.31, 0, 0)$, was confirmed by neutron diffraction for various Si contents on polycrystalline samples (for $x = 0.05$, 0.1, 0.175, 0.25 and 0.5 [18]) and on single crystal samples (for $x = 0.1$, 0.5 and 0.9 [23, 25]). In this work in order to give new insight into the real nature of the magnetic phase transition sequence observed at zero pressure, we correlate the results of macroscopic measurements and neutron diffraction on two samples of $CeRu_2Ge_2$ before and after annealing. A preliminary report was given elsewhere [26].

2. Experimental details

Two single crystals were grown by the Czochralsky pulling method under purified argon atmosphere, starting from high purity elements. Sample 1 was grown in Japan in a tetra-arc furnace, while sample 2 was grown in Grenoble in a tri-arc furnace. Both crystals were large (of the order of 300 mm^3) in order to allow both elastic and inelastic neutron scattering experiments. Sample 1 grew along a direction in the basal plane of the tetragonal structure while sample 2 grew along the c axis. The mosaicity measured by neutron scattering by rocking the samples is of the order of 0.45° for sample 1 and 0.60° for sample 2 (full width at half maximum of a Gaussian lineshape of the (2, 0, 0) Bragg reflection). Small pieces were cut by cleaving and spark cutting for resisitivity and specific heat measurements. After a first study of these as-grown samples, they were all annealed under ultra-high vacuum for 8 days at 950 °C. All the measurements were then repeated.

Resistivity measurements were carried out using the standard four-wire technique with the current i in the basal plane of the tetragonal structure. The leads were glued by silver paint and the measurements were performed down to 1.2 K in a ^{4}He cryostat with a 15 Hz ac bridge with the current i ranging from 10 to 1 mA depending on the temperature. The removal and remake of the electrical leads before and after the annealing operation introduces some errors in the determination of the absolute value of the resistivity. The resistivity data, $\rho(T)$, are thus

normalized to the room temperature resistivity value which is of the order of 45 to 65 $\mu\Omega$ cm throughout all the samples. In the following, the mean value $\rho(300\ \mathrm{K}) = 55\ \mu\Omega$ cm is taken for the normalization.

The specific heat, $C(T)$, was measured on the previously mentioned small pieces using the dynamical adiabatic method down to 300 mK in a ^{3}He cryostat. In this apparatus, measurements are limited to below 8.6 K due to the use of NbTi superconducting wires in the detection chain. To obtain data at higher temperatures, $C(T)$ was then measured in a ^{4}He cryostat on larger pieces of sample with an adiabatic method. A good overlap is obtained between the two set of measurements.

Elastic neutron scattering experiments were performed on the triple-axis spectrometer IN12 at ILL, Grenoble using the fixed final energy mode with $k_F = 1.8\ \mathrm{\AA}^{-1}$ and the collimations 29′–40′–40′–60′. For this spectrometer, higher-order contamination is negligible at this wavevector. The use of a triple-axis spectrometer allows us to achieve a low background due to the energy analysis. A weak signal was indeed expected since previous experiments performed on powder samples show no trace of the antiferromagnetic state [16, 18]. Inelastic neutron scattering experiments were performed on sample 2 before annealing on the same triple-axis spectrometer using this time $k_F = 1.5\ \mathrm{\AA}^{-1}$ and a beryllium filter in order to reduce higher-order contamination. A horizontally focused analyser was used to increase the intensity. The full width at half maximum of the incoherent signal was 0.17 meV in this configuration.

3. Results

3.1. Resistivity

Figure 1 shows the low temperature variation of $\rho(T)/\rho(300\ \mathrm{K})$ for the slice cut from sample 1 before and after annealing. For the as-grown sample, the resitivity exhibits a large drop at $T_C = 7.8$ K as expected from previous results [16, 23]. Above T_C, it only shows a smooth decrease below about 10 K. Accordingly, the derivative $\mathrm{d}\rho(T)/\mathrm{d}T$ shows a peak at T_C but only a continuous decrease above. Annealing induced a huge increase (by almost a factor of four) of the residual resistivity ratio, RRR, $\rho(300\ \mathrm{K})/\rho_0$. Taking $\rho(1.2\ \mathrm{K})$ to be the residual resistivity ρ_0, this quantity evolves from 2.53 $\mu\Omega$ cm before annealing to 0.65 $\mu\Omega$ cm after annealing. In this annealed state, T_N is now marked by an angle in the temperature dependence of ρ (see arrow in figure 1), and thus $\mathrm{d}\rho/\mathrm{d}T$ by a step at 8.3 K. Moreover, although the position of the $\mathrm{d}\rho/\mathrm{d}T$ peak at T_C cannot be perfectly determined, it is obvious that it has been pushed to lower temperature (from about 7.8 K to 7.5 K). The resistivity above T_N is also much lower after annealing.

The slice cut from sample 2 already shows the double transition at $T_C = 7.6$ K and $T_N = 8.15$ K before annealing. Its RRR was better than the slice cut from sample 1. However annealing also improved this value by almost a factor of 2. The corresponding residual resistivities are 1.56 and 0.84 $\mu\Omega$ cm respectively. The effect of annealing is also to increase the splitting $\Delta T = T_N - T_C$. Here T_C remains almost unchanged (7.5 K) but T_N moved to 8.3 K (the same value as for sample 1). The data obtained at low temperatures are shown in figure 2. The derivative of the resistivity is shown for this sample in the inset of figure 2, with the two anomalies at T_N and T_C. After annealing samples 1 and 2 exhibit rather similar behaviour with even close intrinsic values of T_C and T_N which will be discussed later. Results obtained for the transition temperatures are listed in table 1 and the RRRs for each sample are given in table 2. In order to be more quantitative, a complete analysis of the data is presented for sample 2 annealed. Neglecting phonon contribution at low temperatures, the resistivity is fitted from 1.2 to 7 K to the expression

$$\rho = \rho_0 + AT^2 + BT^2 \exp(-\Delta/T) \tag{1}$$

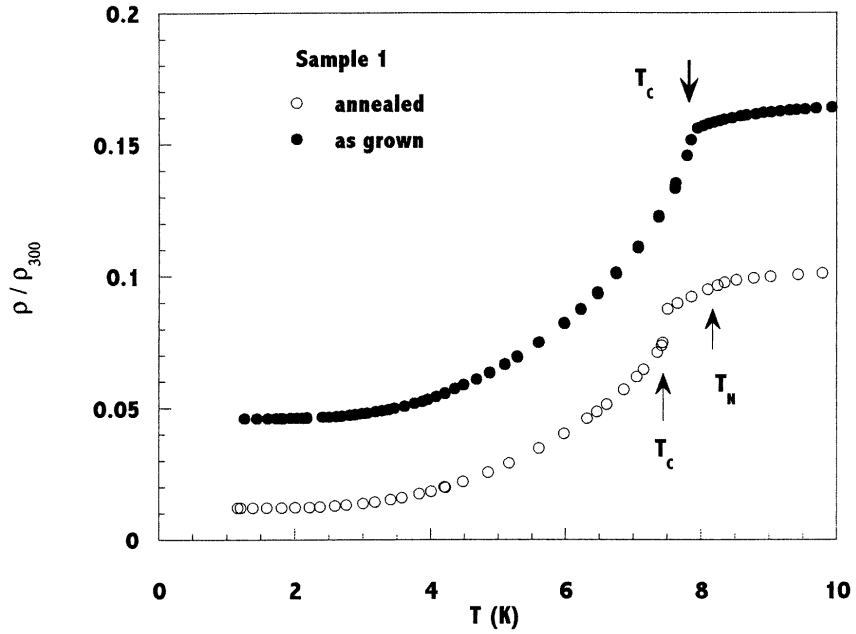

Figure 1. Resistivity of sample 1 as grown and annealed versus temperature. Arrows indicate the magnetic phase transitions.

Table 1. Transition temperatures measured by resistivity, specific heat and neutron scattering.

	Resistivity		Specific heat		Neutron diffraction		
	T_C (K)	T_N (K)	T_C (K)	T_N (K)	T_C (K)	T_N (K)	T_{max} (K)
Sample 1	7.8	—	7.92	—	8	⟨8.5⟩	8
Sample 1 annealed	7.5	8.3	7.60	8.35	7.5	8.3	7.5
Sample 2	7.6	8.15	7.70	8.15	8	8.15	8
Sample 2 annealed	7.5	8.3	7.50	8.30	7.5	8.2	7.5

— means no transition observed, ⟨⟩ means average value of a distribution; numbers are given with the accuracy of the corresponding experimental method. The precision is approximately 1 or 2 on the last digit given.

Table 2. Residual resistivity ratio, specific heat at T_C and antiferromagnetic moment at T_{max}.

	$\rho_{300}/\rho_{1.2}$	C at T_C (J mol^{-1} K^{-1})	m_{AF} (μ_B)
Sample 1	21.7	48	0.1
Sample 1 annealed	83.3	105	1.5
Sample 2	35.7	40	0.5
Sample 2 annealed	66.6	50	1

where ρ_0 is the residual resistivity, the second term corresponds to the electron–electron interaction and the exponential term represents the spin waves scattering of a ferromagnet with a gap Δ in its magnetic excitation spectrum. The value found are $\rho_0 = 0.84(1)\ \mu\Omega$ cm, $A = 0.002(1)\ \mu\Omega$ cm K^{-2}, $B = 0.212(8)\ \mu\Omega$ cm K^{-2} and $\Delta = 8.9(2)$ K, which is consistent with the values found in the literature [20].

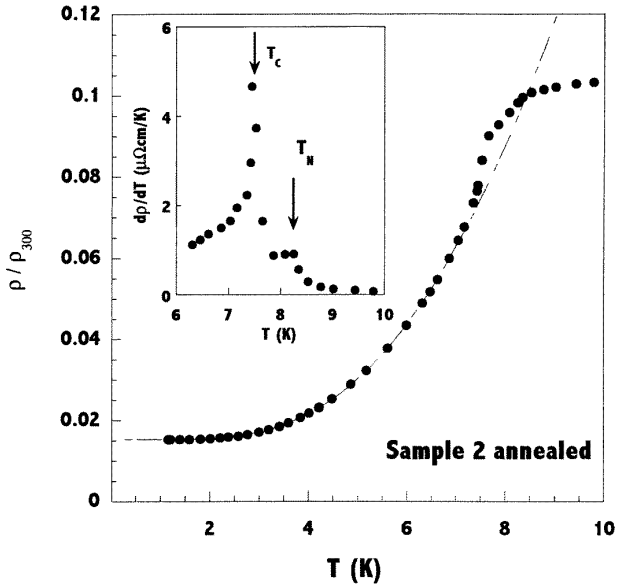

Figure 2. Resistivity of sample 2 annealed versus temperature. The dashed line is a fit to equation (1) given in the text. The inset shows the derivative of this quantity. The arrows show the transition temperatures.

3.2. Specific heat

For both samples the results of the specific heat measurements are in quantitative good agreement for the determination of the transition temperatures and the sample quality with the transport measurements. The transition temperatures obtained are listed in table 1. Beyond the overall agreement, it seems that the ferromagnetic transition temperature of the as-grown samples measured by resistivity is systematically lower than the one determined from specific heat. We take the transition temperatures to be the ones of the specific heat, since the anomalies are better defined for this measurement.

Results obtained on sample 1 at high temperature are compared for the as-grown and annealed sample in figure 3 on a logarithmic scale. The effect of annealing is triple. First, a shoulder appears with a maximum of specific heat at 8.35 K ascribed to the antiferromagnetic ordering. Secondly, the ferromagnetic anomaly is shifted from 7.92 K to 7.60 K. The zigzag observed at 8.47 K for the as-grown sample is an experimental artifact as explained in the experimental details part. Finally, the value of the specific heat at T_C changes from 48 to 105 J mol^{-1} K^{-1}, the shape of the transition being much sharper while the area under the two specific heat anomalies is conserved. These observations are completely consistent with the resistivity measurements.

Concerning sample 2, the antiferromagnetic anomaly is already observed in the as-grown sample. Despite this difference, the scenario is rather similar to the one of sample 1 and the decrease of T_C and the increase of T_N after annealing are well defined and consistent with the resistivity. The measured parameters are listed in tables 1 and 2 for both samples. As for the resistivity, the specific heat after annealing was analysed for sample 2. The data are shown in figure 4 in the range 300 mK–8.6 K. Below the Curie temperature, the specific heat is written

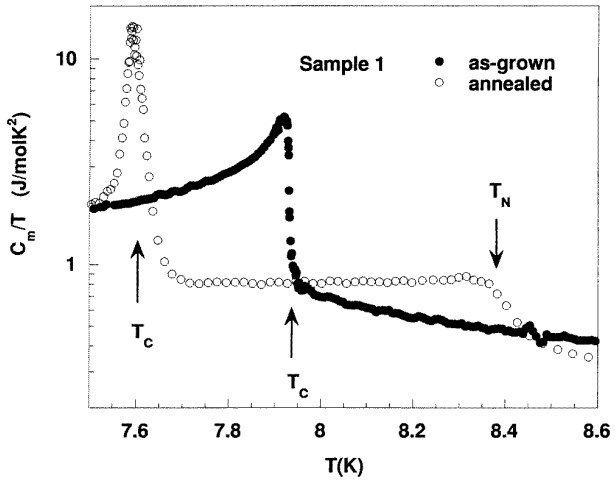

Figure 3. Magnetic specific heat divided by T of sample 1 as grown and annealed plotted on a logarithmic scale versus temperature in the magnetic phase transition region.

using the following expression:

$$C = \gamma T + \beta T^3 + \alpha T^{1.5} \mathrm{e}^{-\frac{\Delta}{kT}}. \tag{2}$$

The first linear term corresponds to the electronic specific heat, the second one is the phonon contribution and the third term often used for gapped ferromagnets corresponds to the spin-wave contribution. The phonon contribution is fixed from the specific heat of the non-magnetic compound $LaRu_2Ge_2$ (taken from [23]) with $\beta = 0.37$ mJ mol^{-1} K^{-4}, which corresponds to a Debye temperature $\theta_D = 175$ K using the simplest equation $\beta = (12\pi^2/5)R/(\theta_D)^3$. The range of the fit is from 300 mK to 7 K. The value of γ is determined from the saturation of C/T at low temperatures with $\gamma = 16.5$ mJ mol^{-1} K^{-2}. Only α and Δ are fitted to (2). The values found are $\alpha = 2.30(8)$ mJ mol^{-1} K$^{-2.5}$ and $\Delta = 10.7(2)$ K. The value of γ is consistent with the quadratic coefficient A of the resistivity for electron–electron interactions. The ratio A/γ^2 is found to be 7×10^{-6} $\mu\Omega$ cm (mol K mJ^{-1})^2, a value in agreement with the known value (10^{-5} $\mu\Omega$ cm (mol K mJ^{-1})^2) after Kadowaki and Woods [27]. The value of the gap is consistent with the one inferred from resistivity measurements albeit higher, but the difference may have a strong fit function dependence. The temperature dependence of the magnetic entropy is shown in the inset of figure 4 for sample 2 annealed. It shows almost a jump at the Curie temperature suggesting a first-order character of this transition while it is like a kink at the Néel temperature. For each sample, the entropy reaches almost the value $R \ln 2$ at 9 K corresponding to the degeneracy of the fundamental crystal-field doublet and indicative of a rather inefficient Kondo screening.

3.3. Neutron scattering

The antiferromagnetic state of $CeRu_2Ge_2$ inferred from the above and previous bulk measurements as well as from similarities with the Si doped alloys [23] is observed for the first time by neutron diffraction in this work. Both crystals (as grown as well as annealed) exhibit a transition at T_N to a long range order. The identified propagation vector is $\boldsymbol{k} = (0.31, 0, 0)$, a robust value observed also in $Ce_{1-x}La_xRu_2Si_2$ [28] and $CeRu_2(Si_{1-x}Ge_x)_2$ [18, 23, 25].

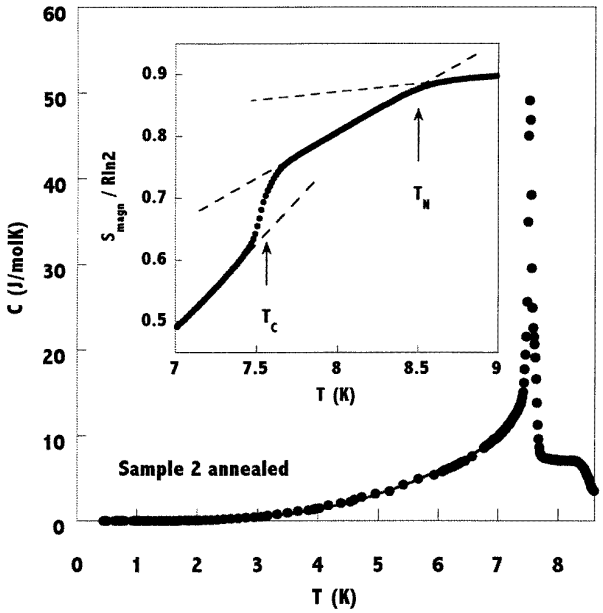

Figure 4. Specific heat of sample 2 annealed versus temperature. The line is a fit to equation (2) given in the text. The inset shows the magnetic entropy of the same sample. The dashed lines indicate the different slopes of the curve.

Since these measurements were performed on a triple-axis spectrometer, only a few satellite reflections were measured and a full refinement of the structure was not made. The structure is thus supposed to be sine-wave modulated by analogy with the other compounds of the family. In the following the magnetic structure is called antiferromagnetic for simplicity and the corresponding order parameter is called the staggered moment. The neutron intensities measured at $\boldsymbol{Q} = (0.7, 1, 0)$ versus temperature for both samples 1 as-grown and annealed are shown in figure 5. For the as-grown one, a distribution of Néel temperatures is observed with a mean value of the order of 8.5 K. The maximum intensity observed at $T = T_{max} = 8$ K corresponds to a magnetic moment of 0.1 μ_B. This value, measured by performing θ–2θ scans around $\boldsymbol{Q} = (0.7, 1, 0)$, is estimated from a comparison with the weak nuclear Bragg reflection (1, 1, 0). We ascribe 1.9 μ_B to this latter reflection in the ferromagnetic state (value of [16]) in order to realize the intensity calibration. This allows us to avoid the difficulty of extinction corrections. An estimate of this effect can be made if we make a calibration from the nuclear intensity of the reflection (1, 1, 0). The 'wrong' value of the ferromagnetic moment is then found to be 1.6 μ_B (another value will be found for a calibration with another nuclear reflection). The small value of the antiferromagnetic moment at T_{max} explains why no anomaly is observed in specific heat and transport measurements for this sample.

After annealing, the distribution of Néel temperature disappears giving rise to a well defined Néel temperature $T_N = 8.3$ K. The magnetic moment, m_{AF}, at $T_{max} = 7.5$ K is approximately 1.5 μ_B. The intensity drops quickly on the ferromagnetic side, which may indicate a first order transition. Concerning sample 2, the antiferromagnetic order was already well defined in the as-grown sample with $T_N = 8.15$ K and a moment at $T_{max} = 8$ K of about 0.5 μ_B. After annealing T_N increases to 8.2 K and the moment at $T_{max} = 7.5$ K is approximately 1 μ_B, a value comparable with the one of sample 1. Surprisingly, the correlation length in

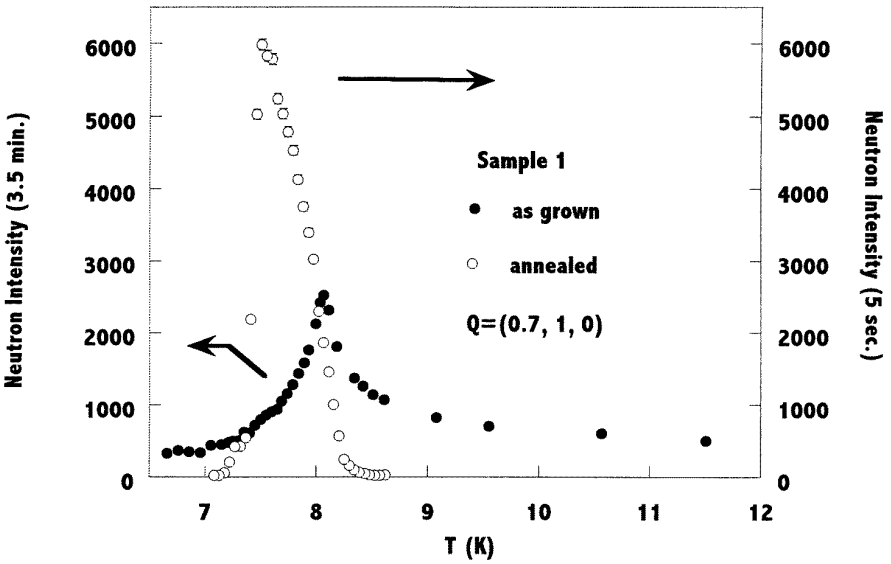

Figure 5. Neutron intensity corresponding to the antiferromagnetic order parameter measured at $Q = (0.7, 1, 0)$ on IN12 for sample 1 as grown and annealed.

the antiferromagnetic state evaluated at T_{max} is found to be almost the same in all the samples studied even for the one with the low staggered moment of 0.1 μ_B. This means that, for this sample, the order is already long range at T_{max}. Concerning the ferromagnetic transition, the Curie temperature equals 8 K for both samples before annealing (T_C being close to T_{max}). This value shifts to 7.5 K after annealing. The ferromagnetic and antiferromagnetic intensities of sample 2 after annealing are shown in figure 6. A fit to the following expression is made:

$$I = I_{BGD} + I_{sat}(1 - T/T_{trans})^{2\beta} \tag{3}$$

where I_{BGD} is the background intensity, I_{sat} is the saturation value of the square of the magnetization, T_{trans} is the transition temperature ($trans = C$ or N) given in the text above and β is the critical exponent of the transition. For the antiferromagnetic transition, a value of 0.40 is found, intermediate between the mean field exponent 0.5 and the renormalized group 3d Ising value 0.31. As usual, this may be due to the large interval of temperature used compared to the theory of phase transition. The value of I_{sat} which is the extrapolation of the antiferromagnetic intensity at $T = 0$ K if the ferromagnetic order did not occur corresponds to about 2.5 μ_B. For the ferromagnetic transition, the statistics is limited due to the underlying nuclear Bragg peak. In this respect T_C is not precisely defined with this measurement. That is why any issue concerning the coexistence of the two magnetic phases (i.e. any quantitative result on the difference between T_C and T_{max}) or the occurrence of a jump of the ferromagnetic order parameter at T_C cannot be addressed here. A fit with (3) is just used as a guide for the eyes for the ferromagnetic order parameter.

Inelastic neutron scattering measurements were also performed. By analogy with $CeRu_2Si_2$ [7] and without any model so far, the dynamical spin susceptibility can be separated into two parts. The first one, independent of the wavevector, is ascribed to the single-site Kondo effect and the second one peaked around some instability wavevectors is ascribed to magnetic correlations. In $CeRu_2Ge_2$, a wavevector independent signal was measured in the paramagnetic phase. Its energy scale is of the order of T_C or T_N (i.e. 1 meV) just above T_N.

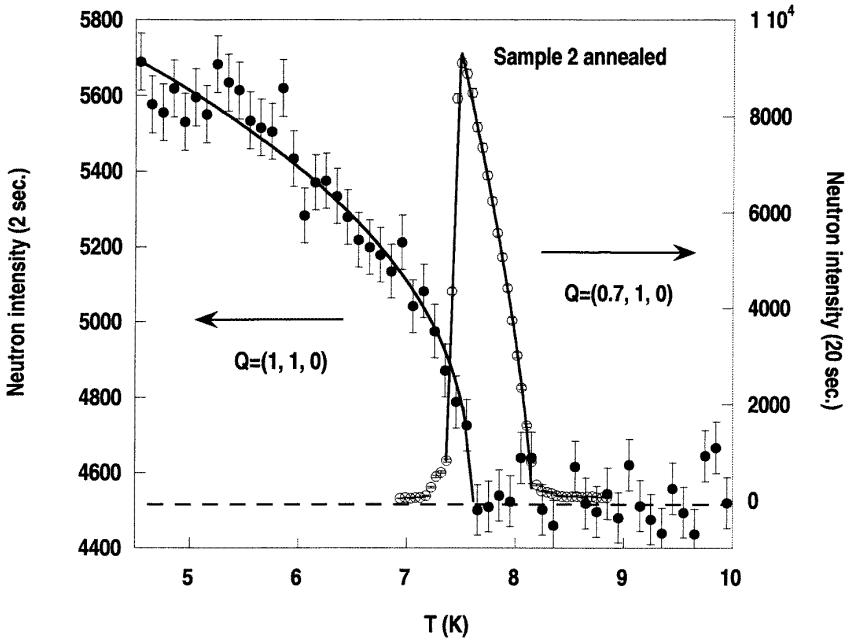

Figure 6. Neutron intensity corresponding to the ferromagnetic and antiferromagnetic order parameters measured at $Q = (1, 1, 0)$ and $Q = (0.7, 1, 0)$ respectively, on IN12 for sample 2 annealed. The dashed line is the background. The line for the ferromagnetic intensity is a guide for the eyes the one for the antiferromagnetic intensity is a fit to equation (3) given in the text.

This signal is completely consistent with previous time-of-flight measurements performed on powder samples [29, 30]. The wavevector dependent fluctuations have a characteristic energy of approximately the instrumental resolution, i.e. 0.1 meV. They are observed up to 30 K near $(1, 1, 0)$ and also near the antiferromagnetic point $(0.7, 1, 0)$ below 12 K. The bottom line is that in the paramagnetic phase, the ferromagnetic fluctuations are dominating but the antiferromagnetic fluctuations appears just above T_N. It is difficult to go deeper in the analysis of the data due to the low energy involved. Finally in the ordered phases, no spin waves are observed in the ferromagnetic phase near $(1, 1, 0)$ and in the antiferromagnetic phase near $(0.7, 1, 0)$ up to 3 meV. This is due to the Ising nature of the system as discussed below.

4. Discussion

The results obtained are summarized in tables 1 and 2. The decrease of the residual resistivity together with the appearance or reinforcement of antiferromagnetism after annealing leads us to the definitive conclusion that the intrinsic behaviour of $CeRu_2Ge_2$ corresponds to the sequence from paramagnetic to modulated and to ferromagnetic order on cooling. Macroscopic and neutron scattering measurements are consistent with each other and especially the absence of the antiferromagnetic resistive and specific heat anomalies for sample 1 as grown is linked to a distribution of Néel temperatures in this sample. An antiferromagnetic order parameter was also recently found in μSR experiments performed on powder samples [31]. In figure 7, the antiferromagnetic order parameter measured at T_{max} is shown versus the inverse RRR. These two quantities are the ones which have the strongest variation over all the measured parameters

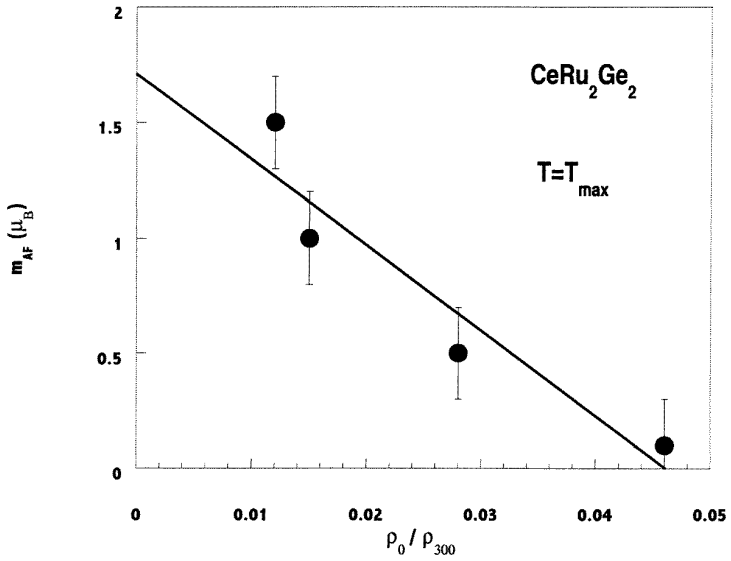

Figure 7. Antiferromagnetic moment, m_{AF}, measured at $\boldsymbol{Q} = (0.7, 1, 0)$ for $T = T_{max}$ versus the inverse resistivity ratio. Each point corresponds to one sample (sample 1 and 2 before and after annealing). The line is a fit to equation (4) given in the text.

in the four samples considered. The antiferromagnetic order parameter is indeed the most fragile against disorder. In the simplest model of the influence of disorder on magnetism used for example for alloys of transition metals [32], the magnetic moment m (starting from a pure compound with a moment m_{matrix}) of an alloy with a concentration c of impurities and a number of electrons Z is

$$m = m_{matrix} - Zc\mu_B. \tag{4}$$

By generalizing this approach to the disorder found here before and after annealing (e.g. inversion between Ru and Ge, stacking faults, ... [33]) and taking the residual resistivity to be proportional to the disorder concentration c, a linear fit to the antiferromagnetic moment measured at T_{max} gives a value of $m_{matrix} = 1.7\ \mu_B$ obtained for an ideally pure sample (see solid line in figure 7). Although the model may be inadequate or too simple, the underlying physics seems well defined. The next quantity showing strong variation among the samples studied is the maximum of specific heat at T_C (see table 2). Despite the fact that this quantity changes substantially after annealing, the ferromagnetic moment does not change in any of the samples because the area of the transition, to which it is proportional, in a mean field picture, is conserved.

This sequence of magnetic transitions, albeit unique in the 1–2–2 Ce intermetallic family, is well known in the study of the so called Lifshitz point and/or in the ANNNI (anisotropic next-nearest-neighbour Ising) model, a pure spin model for which no Kondo effect is included [34]. Pressure studies may indicate the proximity of such a tricritical point where the ferromagnetic, modulated and paramagnetic phases meet and, finally, only a transition from a paramagnetic to a ferromagnetic state occurs at an extrapolated negative pressure around $P = -1$ GPa. Such a point may in principle be reached for a larger volume of the unit cell as in $CeRu_2Sn_2$, a compound not yet satisfactory synthesized. In principle, in such a model, the propagation

vector changes continuously with P in the vicinity of such a point. This is not the case in our system since the value $\boldsymbol{k} = (0.31, 0, 0)$ is quite robust in this family of compounds; it may be associated with Fermi surface peculiarities [35]. Albeit the evolution of $\boldsymbol{k}$ with pressure is not known in $CeRu_2Ge_2$ [36], its constant value is *a priori* known from the phase diagram matching with the Si doped compounds. The interesting point is that in this framework, the transition from paramagnetic to modulated is second order and the transition from modulated to ferromagnetic is first-order in tetragonal symmetry [37]. The first-order nature of the ferromagnetic transition seems to be verified in our compound from the asymmetry of the antiferromagnetic order parameter (almost a discontinuous drop below T_{max}), the quasi-jump in the entropy and in the thermal expansion [38]. For sample 2, the annealing operation produces an increase of the difference ΔT between the Curie temperature and the Néel temperature. It is then interesting to correlate the value of the maximum staggered magnetization m_{AF} and the splitting $\Delta T = T_N - T_C$. In the simplest model of such a transition [37], the relation between the staggered magnetization, the uniform magnetization, the Néel and Curie temperatures is

$$m_{AF} \approx m_F \sqrt{\frac{T_N}{T_C} - 1}. \tag{5}$$

If we assume a value of the ferromagnetic moment m_F of 1.9 μ_B, the value of ΔT measured before and after annealing will give a magnetic moment m_{AF} of 0.4 and 0.9 μ_B respectively, which are in fairly good agreement with our measurements keeping in mind the crude estimate made in our neutron scattering data analysis. Relation (5) can be seen as phenomenological and thus does not imply the occurence of a tricritical point.

The spin waves were not observed either in the antiferromagnetic nor in the ferromagnetic phase where they are expected from the bulk measurements with a gap of approximately 1 meV. This is ascribed to the strong Ising nature of the fundamental crystal field doublet which is an almost pure $|\pm 5/2\rangle$ state. On the other hand, longitudinal gapped and dispersive excitation were observed in $CeRu_2SiGe$ at the wavevector $\boldsymbol{Q} = (0.3, 0.3, 0)$ which is not the ordering vector [39]. These excitation are observed when the order parameter squares up, i.e. when higher-order harmonics are observed in neutron diffraction experiments. No such harmonics and such excitations were observed in our compound. For $CeRu_2SiGe$, these excitations account for the 'spin waves' put forward in the interpretation of the bulk measurements but unlikely to exist for an Ising ground state. The ground state is in fact $\alpha|+/-5/2\rangle + \beta|-/+3/2\rangle$ giving a measured magnetic moment, m_F, of 1.76 μ_B [18] or 1.9 μ_B [16] depending of the estimates. The theoretical saturation value, m_{sat}, ($m_{sat} = 6/7[5/2\alpha_2 - 3/2\beta_2]$), is very sensitive to α, an estimate of which is 0.94 [18] or 0.98 [19] from inelastic neutron scattering (crystal field spectroscopy) giving a moment of 1.79 and 2.01 μ_B respectively. In the four samples we studied, there is a distribution of 10% of the ferromagnetic moment which is within the error bars for the experimental method we used; this is why we fixed the zero temperature ferromagnetic moment, m_F, to the value $m_{sat} = 1.9\ \mu_B$. This value, m_{sat}, is thus the maximal moment that can be found in this compound at $T = 0$ K. In this respect, the value of m_{AF} found at T_{max} 8 K, that is 1.5 μ_B for the best sample and 1.7 μ_B for the ideally good sample (see figure 7) is consistent with m_{sat}. From T_{max} to $T = 0$ K, there is indeed a temperature range in which the magnetic moment can increase from m_{AF} to m_{sat}. We can thus conclude that if the compound were antiferromagnetic, m_{AF} would probably reach m_{sat} at $T = 0$ K as m_F actually does.

Let us discuss the 'light' heavy fermion nature of $CeRu_2Ge_2$. Taking for the Kondo temperature a value of 1 K which seems to be the residual low temperature neutron linewidth Γ (extrapolation of the data to zero temperature), we expect a huge value of the linear coefficient of the specific heat γ_0 ($\gamma_0 \sim 1/T_K$) of the order of 1000 mJ mol^{-1} K^{-2}. In fact the ferromagnetic

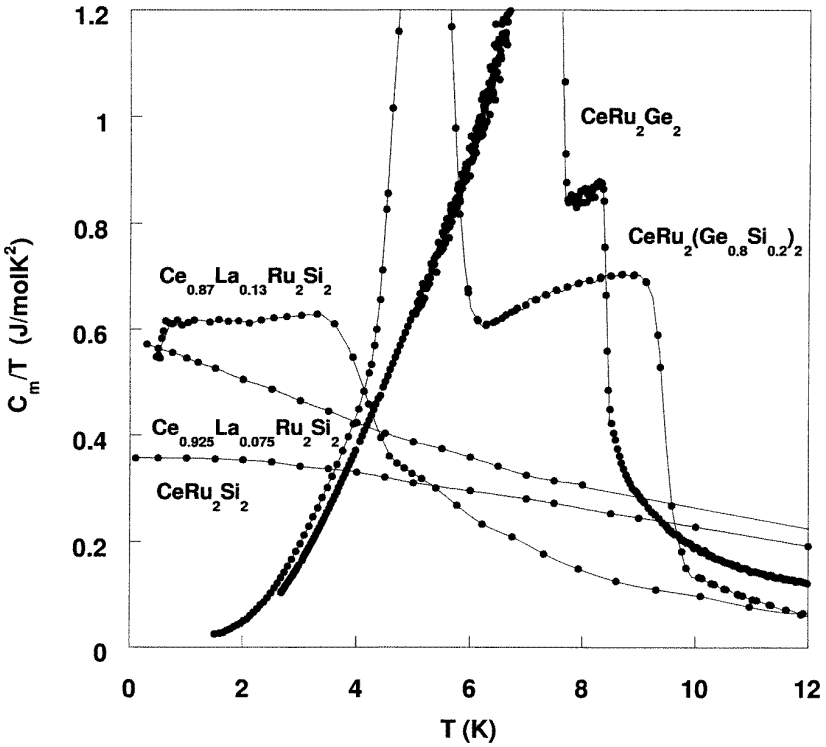

Figure 8. Magnetic specific heat divided by T versus temperature for $CeRu_2Si_2$, $Ce_{0.925}La_{0.075}Ru_2Si_2$, $Ce_{0.87}La_{0.13}Ru_2Si_2$ [6, 41, 42], $CeRu_2(Ge_{0.8}Si_{0.2})_2$ [23] and $CeRu_2Ge_2$ (sample 1 annealed). Lines are guides for the eyes.

molecular field H_m acts as an external magnetic field and reduces γ_0 to γ. A phenomenological relation inspired from the one used for $CeCu_6$ under magnetic field [40] is

$$\gamma = \gamma_0/(1 + \eta\gamma_0^2 H_m^2) \tag{6}$$

where η is a dimensionless factor of the order of unity if H_m and γ_0 are expressed in reciprocal units of each other. Taking $m_F H_m \sim k_B T_C \sim 10$ K and $\eta\gamma_0^2 \sim 1/T_K^2$ with $T_K \sim 1$ K and with the expected value of γ_0, we found that γ is reduced to 10 mJ mol^{-1} K^{-2}, consistently with the measured value of 16.5 mJ mol^{-1} K^{-2}. It is worthwhile to note that this argument is linked with a peculiarity of the single-site neutron scattering linewidth Γ. This latter is not field dependent in heavy fermion compounds (e.g. $CeCu_6$, $CeRu_2Si_2$) studied up to now under high magnetic field [7, 8]. In other words the usual scaling between $1/\Gamma$ and γ is not true under magnetic field. That is why, extrapolating this behaviour for a molecular field, we took $\gamma_0 \sim 1/\Gamma$.

It is worthwhile to underline the shape of the specific heat anomaly. If we consider the temperature variation of C/T between T_N and T_C, it is nearly constant (although a weak decrease will probably occur on a larger temperature range) and equals $\gamma_0 \sim 1$ J mol K^2 for the best sample, i.e. sample 1 annealed. This flattening on cooling is quite similar to that observed for the *weakly* antiferromagnetic compound $Ce_{1-x}La_xRu_2Si_2$ for $x = 0.1$ and $x = 0.13$ [41] located just on the magnetic side of the QCP (corresponding to $x_c = 0.08$ [6]).

Here between T_N and T_C, C/T is just above the critical value $\gamma_c \sim 600$ mJ mol^{-1} K^{-2} found for $x = x_c$. The entrance in the ferromagnetic state will lead to a drop of C/T from γ_0 to $\gamma = 16.5$ mJ mol^{-1} K^{-2}. On the other hand, for sample 1 as-grown, there is no anomaly at T_N but a continuous increase of C/T between T_N and T_C (see figure 3). This is rather similar to the behaviour found, this time, for the *nearly* antiferromagnetic compound where $x = x_c - \varepsilon$. For all these mentioned cases, C/T is shown comparatively in figure 8 for the Pauli paramagnet $CeRu_2Si_2$ [6], the nearly antiferromagnetic compound $Ce_{0.925}La_{0.075}Ru_2Si_2$ [42], the weakly antiferromagnetic compound $Ce_{0.87}La_{0.13}Ru_2Si_2$ [41], $CeRu_2Ge_2$ studied here (sample 1 annealed) and $CeRu_2(Ge_{0.8}Si_{0.2})_2$ [23]. For $CeRu_2Ge_2$, as the entropy conservation precludes such a large constant C/T term down to 0 K for such a high characteristic temperature ($T_N \sim 8$ K), a correlated change in magnetic and electronic structure occurs. An appealing picture is that, in the antiferromagnetic phase, the 4f electrons appear itinerant with a Fermi surface similar to the one of $CeRu_2Si_2$ which explains the persistence of the instability wavevector $\boldsymbol{k}$ in the antiferromagnetic phase of $CeRu_2Ge_2$. Below T_C, the 4f electrons appear localized with a Fermi surface quite similar to that of $CeRu_2Si_2$ in the polarized phase. Under pressure reaching the QCP at P_c (8.7 GPa) in $CeRu_2Ge_2$, the ferromagnetic ground state collapses far below P_c (at $P \sim 3.5$ GPa [20]) and the QCP corresponds to a transition from antiferromagnetic to paramagnetic state. Physically the pressure will decrease the value of C/T as T_C collapses. The maximum of C/T, namely γ_c, will coincide with the QCP. The consistency of the results in the $CeRu_2Ge_2$ and $CeRu_2Si_2$ families with their known electronic properties (Fermi surface) urges theoretical development.

5. Conclusion

We showed that the intrinsic behaviour of $CeRu_2Ge_2$ is to exhibit the sequence of transition from a paramagnetic to a modulated and finally a ferromagnetic state. The first transition is second order while the second one is first order. The antiferromagnetic moment increases up to 1.5 μ_B after annealing, a value consistent with the splitting between the Curie temperature and the Néel temperature and the expected maximum moment for this ground state. This value is very sensitive to disorder and decreases linearly with the increase of the residual resistivity. The different magnetic states of $CeRu_2Ge_2$ are directly related with the nature of the localization or the itineracy of the 4f Ce electrons.

Acknowledgments

We thank H Wilhelm, B Revaz, G Santi and D Jaccard of University of Geneva for helpful discussions. D Raoelisson and M Fougères are acknowledged for performing some of the measurements as part of their university training. Part of the data was analysed during a stay at University of Geneva where one of us (SR) is supported by the Swiss National Science Foundation.

References

[1] Millis A J 1993 *Phys. Rev.* B **48** 7183
[2] Moriya T and Takimoto T 1995 *J. Phys. Soc. Japan* **64** 960
[3] Aeppli G and Broholm C 1994 *Handbook on the Physics and Chemistry of Rare Earths* vol 19, ed K A Gschneidner Jr, L Eyring, G H Lander and G R Choppin (Amsterdam: Elsevier)
[4] Haen P, Flouquet J, Lapierre F, Lejay P and Remenyi G 1987 *J. Low Temp. Phys.* **67** 391
[5] Paulsen C, Lacerda A, Puech L, Haen P, Lejay P, Tholence J L, Flouquet J and de Visser A 1990 *J. Low Temp. Phys.* **81** 317

[6] Flouquet J, Kambe S, Regnault L P, Haen P, Brison J P, Lapierre F and Lejay P 1995 *Physica* B **215** 77 and references therein
[7] Rossat-Mignod J, Regnault L P, Jacoud J L, Vettier C, Lejay P, Flouquet J, Walker E, Jaccard D and Amato C 1988 *J. Magn. Magn. Mater.* **76/77** 376
[8] Raymond S, Regnault L P, Kambe S, Lejay P and Flouquet J 1998 *J. Phys.: Condens. Matter* **10** 2363
[9] Grier B H, Lawrence J M, Murgai V and Parks R D 1984 *Phys. Rev.* B **29** 2664
[10] Aoki H, Ujii S, Albessard A K and Onuki Y 1993 *Phys. Rev. Lett.* **71** 2110
[11] Tautz F, Julian S R, McMullan G J and Lonzarich G G 1995 *Physica* B **206/207** 29
[12] King C A and Lonzarich G G 1991 *Physica* B **171** 161
[13] Ikezawa H, Aoki H, Takashita M, Haworth C J, Uji S, Terashima T, Maezawa K, Settai R and Onuki Y 1997 *Physica* B **237/238** 210
[14] Rietschel H, Renker B, Felten R, Steglich F and Weber G 1988 *J. Magn. Magn. Mater.* **76/77** 105
[15] Böhm A, Caspary R, Habel U, Pawlak L, Zuber A, Steglich F and Loidl A 1988 *J. Magn. Magn. Mater.* **76/77** 150
[16] Besnus M J, Essaihi A, Hamdaoui N, Fisher G, Kappler J P, Meyer A, Pierre J, Haen P and Lejay P 1991 *Physica* B **171** 350
[17] Thompson J D, Uwatoko Y, Graf T, Hundley M F, Mandrus D, Godart C, Gupta L C, Canfield P C, Migliori A and Borges H A 1994 *Physica* B **199/200** 589
[18] Dakin S, Rapson G and Rainford B D 1992 *J. Magn. Magn. Mater.* **108** 117
[19] Loidl A, Knorr K, Knopp G, Krimmel A, Caspary R, Böhm A, Sparn G, Geibel C, Steglich F and Murani A P 1992 *Phys. Rev.* B **46** 9341
[20] Wilhelm H, Alami-Yadri K, Revaz B and Jaccard D 1999 *Phys. Rev.* B **59** 3651
Wilhelm H and Jaccard D 1998 *Solid State Commun.* **106** 239
[21] Kobayashi T C, Miyazu T, Shimizu K, Amaya K, Kitaoka Y, Onuki Y, Shirase M and Takabatake T 1998 *Phys. Rev.* B **57** 5025
[22] Süllov S, Aronson M C, Rainford B D and Haen P 1999 *Phys. Rev. Lett.* **82** 2963
[23] Haen P, Mallmann F, Besnus M J, Kappler J P, Bourdarot F, Burlet P and Fukuhara T 1996 *J. Phys. Soc. Japan* **65** (Supplement B) 16 and references therein
[24] Haen P, Bioud H and Fukuhara T 1999 *Physica* B **259–261** 85
[25] Mignot J M, Regnault L P, Jacoud J L, Rossat-Mignod J, Haen P and Lejay P 1991 *Physica* B **171** 357
[26] Raymond S, Raoelison D, Kambe S, Regnault L P, Fåk B, Calemczuk R, Flouquet J, Haen P and Lejay P 1999 *Physica* B **259–261** 48
[27] Kadowaki K and Woods S B 1986 *Solid State Commun.* **58** 507
[28] Quézel S, Burlet P, Jacoud J L, Regnault L P, Rossat-Mignod J, Vettier C, Lejay P and Flouquet J 1988 *J. Magn. Magn. Mater.* **76/77** 403
[29] Rainford B D, Dakin S and Severing A 1992 *J. Magn. Magn. Mater.* **108** 119
[30] Rainford B D, Neville A J, Adroja D T, Dakin S J and Murani A P 1996 *Physica* B **223/224** 163
[31] Henning Walf G, Mienert D, Klauß H H, Kopmann W, Wagener W, Lietterst F J, Fontes M B, Bud'ko S L and Baggio-Saitovitch E 1998 private communication
[32] See e.g. Friedel J 1958 *Nuovo Cimento Suppl.* **7** 287
Mott N F and Jones H 1936 *Metals and Alloys* (Oxford: Clarendon) p 286
[33] Vernière A, Lejay P, Boucherle J X, Muller J, Raymond S, Flouquet J and Sulpice A 1995 *Physica* B **206/207** 509
[34] For a review see e.g. Shapira Y 1994 *Multicritical Phenomena* ed R Pynn and A Skeltop (New York: Plenum)
[35] Miyako Y, Takeuchi T, Taniguchi T, Yamamoto Y, Kawarazaki S, Acet M, Dumpich G and Wassermann E F 1996 *Z. Phys.* B **101** 339
[36] Preliminary experiments performed up to 4 kbar at ILL, Grenoble, by B D Rainford, G McIntyre, S Süllov and P Haen, show that $\boldsymbol{k}$ does not change in this pressure range
[37] Michelson A 1977 *Phys. Rev.* B **16** 577
[38] Bioud H 1998 *Thèse de l'Université Joseph Fourier* Grenoble
[39] Rainford B D, Adroja D T, Haen P, Fåk B and Fukuhara T 1998 private communication
[40] Amato A, Jaccard D, Flouquet J, Lapierre F, Tholence J L, Fisher R A, Lacy S E and Olsen J A 1987 *J. Low Temp. Phys.* **68** 71
[41] Fisher R A, Marcenat C, Phillips N E, Haen P, Lapierre F, Lejay P, Flouquet J and Voiron J 1991 *J. Low Temp. Phys.* **84** 49
[42] Kambe S, Flouquet J and Hargreaves T 1997 *J. Low Temp. Phys.* **108** 383